Available online at www.sciencedirect.com
SCIENCE DIRECT®
Biochimica et Biophysica Acta 1696 (2004) 103–111
BIOCHIMICA ET BIOPHYSICA ACTA
BBA
www.bba-direct.com

Structure of the D142N mutant of the family 18 chitinase ChiB from *Serratia marcescens* and its complex with allosamidin

Gustav Vaaje-Kolstad[a], Douglas R. Houston[b], Francesco V. Rao[b], Martin G. Peter[c], Bjørnar Synstad[a], Daan M.F. van Aalten[b], Vincent G.H. Eijsink[a,*]

[a] *Department of Chemistry and Biotechnology, Agricultural University of Norway, P.O. Box 5040, N-1432 Aas, Norway*
[b] *Wellcome Trust Biocentre, School of Life Sciences, University of Dundee, Dundee DD1 5EH, Scotland, UK*
[c] *Institute of Chemistry, University of Potsdam, P.O. Box 601553, D-14415 Potsdam, Germany*

Received 18 July 2003; received in revised form 16 September 2003; accepted 23 September 2003

Abstract

Catalysis by ChiB, a family 18 chitinase from *Serratia marcescens*, involves a conformational change of Asp142 which is part of a characteristic $D_{140}XD_{142}XE_{144}$ sequence motif. In the free enzyme Asp142 points towards Asp140, whereas it rotates towards the catalytic acid, Glu144, upon ligand binding. Mutation of Asp142 to Asn reduced k_{cat} and affinity for allosamidin, a competitive inhibitor. The X-ray structure of the D142N mutant showed that Asn142 points towards Glu144 in the absence of a ligand. The active site also showed other structural adjustments (Tyr10, Ser93) that had previously been observed in the wild-type enzyme upon substrate binding. The X-ray structure of a complex of D142N with allosamidin, a pseudotrisaccharide competitive inhibitor, was essentially identical to that of the wild-type enzyme in complex with the same compound. Thus, the reduced allosamidin affinity in the mutant is not caused by structural changes but solely by the loss of electrostatic interactions with Asp142. The importance of electrostatics was further confirmed by the pH dependence of catalysis and allosamidin inhibition. The pH-dependent apparent affinities for allosamidin were not correlated with k_{cat}, indicating that it is probably better to view the inhibitor as a mimic of the oxazolinium ion reaction intermediate than as a transition state analogue.

Keywords: Chitinase; Mutagenesis; Allosamidin; Inhibitor; *Serratia marcescens*

1. Introduction

Chitinases catalyse the hydrolysis of chitin, a biopolymer of β(1–4)-linked *N*-acetylglucosamine. These enzymes belong to two families of glycoside hydrolases, namely family 18 and family 19 [1]. The catalytic domains of family 18 chitinases have a TIM-barrel ($(\beta\alpha)_8$ barrel) fold. The β-strand four of the TIM-barrel contains a characteristic DXDXE sequence motif that includes the glutamate residue that protonates the oxygen in the scissile glycosidic bond [2–6]. One well-studied member of this family of enzymes is Chitinase B (ChiB) from the soil bacterium *Serratia marcescens*. ChiB is an exochitinase that degrades chitin chains from their non-reducing ends [7,8]. In addition to the catalytic domain, this enzyme has a small chitin-binding domain that extends the substrate-binding cleft towards the reducing end of the polysaccharide chain [8].

Catalysis in family 18 chitinases involves the *N*-acetyl group of the sugar bound in the −1 subsite of the enzyme ([2–6]; Fig. 1). Protonation of the glycosidic bond and leaving group departure are accompanied by nucleophilic attack by the carbonyl oxygen of the *N*-acetyl group on the anomeric carbon, thus yielding an oxazolinium ion intermediate ([2–6]; Figs. 1C and 2A). The formation of this type of intermediate has also been described for *N*-acetyl-β-hexosaminidases [9,10]. Catalysis in family 18 chitinases involves conserved residues in the DXDXE motif, which in case of ChiB are the catalytic acid, Glu144, as well as Asp142 and Asp140 [6,11]. Structural studies have shown that the side chain of Asp142 (and its equivalents in other family 18 chitinases) may occur in two conformations, either pointing "down" into the TIM barrel (towards Asp140) or pointing "up" towards Glu144 (Fig. 1; [5,6,11–13]). Binding of substrate fixes the Asp142 side chain in the "up" position, which is of importance for substrate-distortion and catalysis (see Fig. 1 and below).

* Corresponding author. Tel.: +47-6494-9472; fax: +47-6494-7720.
E-mail address: vincent.eijsink@ikb.nlh.no (V.G.H. Eijsink).

1570-9639/$ - see front matter © 2003 Elsevier B.V. All rights reserved.
doi:10.1016/j.bbapap.2003.09.014

Asp142 is important for catalysis since its mutation to alanine in ChiB (see below) and other family 18 chitinases [12] abolishes enzyme activity. Replacement with Asn also reduces activity, but to a lesser extent [6,14,15]. The D142N mutant is interesting because its considerable residual activity indicates that catalysis still proceeds via a wild-type-like mechanism. On the other hand, this mutant and an analogous mutant in another family 18 chitinase [14] show distinct changes in their pH–activity profiles.

To gain further insight into the contribution of Asp142 to catalysis and to study possible structural effects of the D142N mutation we have determined the crystal structure of the ChiB mutant. In addition, enzymological and structural studies have been conducted with allosamidin, a pseudotrisaccharide that is known to inhibit family 18 chitinases [5,6,11,16]. Allosamidin is structurally similar to the proposed reaction intermediate (Fig. 2) and its high affinity for family 18 chitinases has led to the suggestion that the inhibitor is a transition state analogue [3–6,11,17].

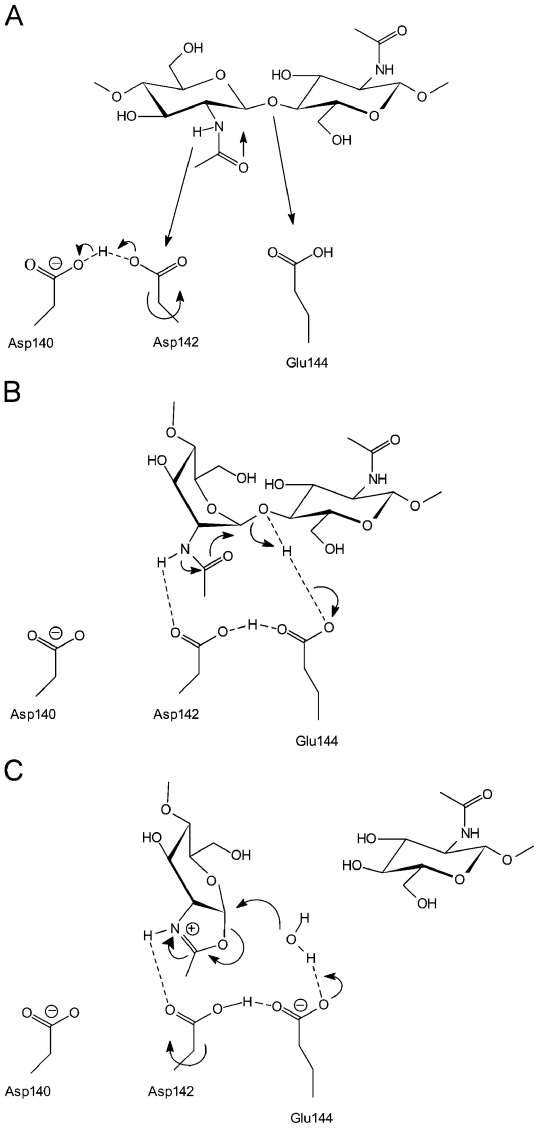

Fig. 1. Catalytic mechanism of family 18 glycoside hydrolases. The figure shows the mechanism proposed in Ref. [4] and further elaborated in Ref. [6]. (A) Substrate-binding. (B) Substrate distortion and protonation of the glycosidic bond. (C) Formation of the oxazolinium ion intermediate and leaving group departure; a water molecule (destined to hydrolyse the oxazolinium ion) is approaching the anomeric carbon.

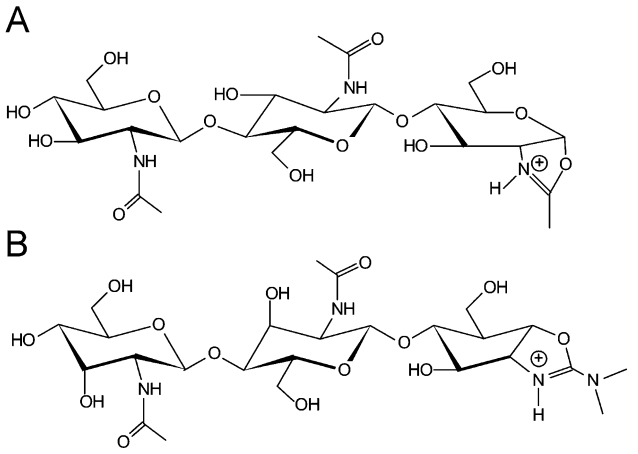

Fig. 2. The oxazolinium ion and allosamidin. (A) The proposed positively charged reaction intermediate (oxazolinium ion). (B) Allosamidin.

2. Materials and methods

2.1. Mutagenesis, protein purification and crystallization

The ChiB D142N mutant was produced by site directed mutagenesis using the Stratagene QuickChange kit (Stratagene, La Jolla, CA) and was overexpressed and purified as previously described [7]. The pure protein was lyophilised, dissolved to 1.0 mg/ml in 25 mM Tris–HCl, pH 8.0, dialyzed overnight in the same buffer and concentrated to 10 mg/ml with Ultrafree-MC concentration tubes with a 10,000 M_W cut-off (Millipore, Bedford, MA, USA). Subsequently, hanging drop vapour diffusion experiments were set up for crystallization. Crystals appeared within days in 100 mM HEPES pH 7.0, 10–20% glycerol and 1.0–1.5 M ammonium sulfate. The crystallization condition used for producing crystals for data collection was 100 mM HEPES pH 7.0, 15% glycerol and 1.3 M ammonium sulfate. Crystals were soaked with allosamidin (kindly provided by G. Gooday) to a final concentration of 10 mM to yield the D142N–allosamidin complex. Prior to data collection, the crystals were cryoprotected by immersion in mother liquor containing 25% glycerol and frozen in a nitrogen cryostream.

2.2. Structure determination

Data for the D142N mutant and the D142N–allosamidin complex were collected on a Rigaku rotating anode and on beamline ID14EH1 at the European Synchrotron Radiation

Facility in Grenoble, respectively, in cryogenic conditions. The data were processed using DENZO and scaled using SCALEPACK from the HKL suite [18]. The previously published structure of the D140N ChiB mutant [19] was used as template for an initial rigid body refinement for the D142N ChiB structure. ChiB wild-type in complex with allosamidin [6] was used as template for an initial rigid body refinement for the D142N–allosamidin complex structure. Iterative model building was performed in O [20] together with refinement in CNS [21], which included simulated annealing. The molecular topology and starting structure of allosamidin were created using the PRODRG server [22]. Allosamidin was not included in the refinement until well defined by the unbiased $|F_o| - |F_c|$, ϕ_{calc} electron density. Both structures have two monomers (A and B) in the asymmetric unit related to each other by a 2-fold non-crystallographic axis. As observed previously for other ChiB structures, the two monomers were essentially identical (RMSD = 0.368 Å), the only difference being a limited number of alternate side chain conformations for surface residues (and for residue 142; see Results). In this study, we have consistently used the B-monomer for structural comparison. Hydrogen bond analysis was carried out with WHAT IF [23] using the HB2 algorithm [24]. Structure superpositions were made with LSQKAB [25] from the CCP4 suite [26] based on Cα atoms.

2.3. Enzymology

The activities of ChiB variants were determined using 4-methylumbelliferyl-β-D-*N*,*N*′ -diacetylchitobioside (Sigma, St. Louis, USA) as substrate, essentially as described previously [7]. In a standard assay for determination of specific activity, 50 μl of a mixture containing enzyme (at appropriate concentration), 20 μM substrate, 50 mM citrate-phosphate buffer pH 6.3 and 0.1 mg/ml BSA was incubated at 37 °C. After 10 min, the reaction was stopped by adding 1.95 ml of an aqueous 0.2 M Na_2CO_3 solution. Fluorescence of the liberated 4-methylumbelliferol anion was measured using a DyNA 200 Fluorimeter (Hoefer Pharmacia Biotech, San Francisco, CA). In order to prevent substrate inhibition the substrate concentration was in the same range as the K_m of the substrate [7]. Thus, changes in specific activity to some extent reflect changes in K_m (if these occur; see Results).

Kinetic parameters were determined by initial rate measurements at various substrate concentrations. Enzyme activity was found to be constant for at least 10 min in all situations, meaning that the determination of initial rates was straightforward. Because of limitations caused by the sensitivity of the assay and by substrate inhibition, the range of substrate concentrations was relatively narrow (5–40 μM). As previously shown [7], ChiB displays normal steady-state kinetics in this substrate range and the activity measurements are sufficiently accurate to determine kinetic parameters with acceptable error margins. K_m and k_{cat} values were determined on the basis of 8–12 independent rate measurements (or 2–3 per substrate concentration) using the hyperbolic regression option provided by Hyper (copyright 1992–1996, J.S. Easterby, obtainable from homepage:http://homepage.ntlworld.com/john.easterby).

Variation in pH was achieved by using the following buffers: 50 mM citrate-phosphate pH 4.2, pH 5.4, pH 6.3 and pH 7.2, 50 mM Tris–HCl pH 8.0, 50 mM ethanolamin-HCl pH 9.0 and pH 10.0. These buffers were chosen after it had been established that the variation in buffer ions did not affect catalytic activity.

IC_{50} values of allosamidin for ChiB and the D142N mutant were determined under standard assay conditions using enzyme concentrations of 2.5 and 73 nM, respectively, a substrate concentration of 20 μM, and varying concentrations of the inhibitor. IC_{50} values were estimated by plotting the relative specific activity as function of the inhibitor concentration.

Protein concentrations were determined using the Bio-Rad Protein Assay (Bio-Rad, Hercules, CA, USA), with bovine serum albumin as a standard.

3. Results

3.1. The D142N structure

The D142N structure was refined to 1.85 Å with *R*-factors converging to $R = 0.159$ and $R_{free} = 0.194$ (Table 1).

Table 1
Refinement and structure quality statistics for the D142N and D142N–allosamidin structures

	D142N	D142N–allosamidin
Resolution (Å)	15.0–1.85	25.0–1.97
Number of reflections measured	272578 (16366)	240744 (19590)
Number of unique reflections	90699 (7656)	74700 (6790)
Redundancy	3.0 (2.1)	3.2 (2.9)
Mean $I/\sigma I$	31.5 (8.1)	21.7 (3.0)
Completeness (%)	96.7 (82.7)	95.3 (87.9)
R_{merge}	0.038 (0.12)	0.043 (0.33)
Space group	$P2_12_12_1$	$P2_12_12_1$
Unit cell parameters (Å)	$a = 55.95$	$a = 55.87$
	$b = 103.98$	$b = 104.74$
	$c = 186.46$	$c = 186.73$
Number of protein atoms	7884	7831
Number of solvent waters	1287	861
Number of glycerol molecules	24	6
Number of SO_4 molecules	7	1
Number of inhibitor molecules	–	2
R_{cryst}	0.159	0.189
R_{free}	0.194	0.230
Number of R_{free} reflections	1321	732
RMSD from ideal geometry		
bonds (Å)	0.016	0.011
angles (°)	1.7	1.5
Average main chain B (Å^2)	16.8	31.0

Values in parentheses are for the outer shell. No σ cutoff was applied to the data used for refinement.

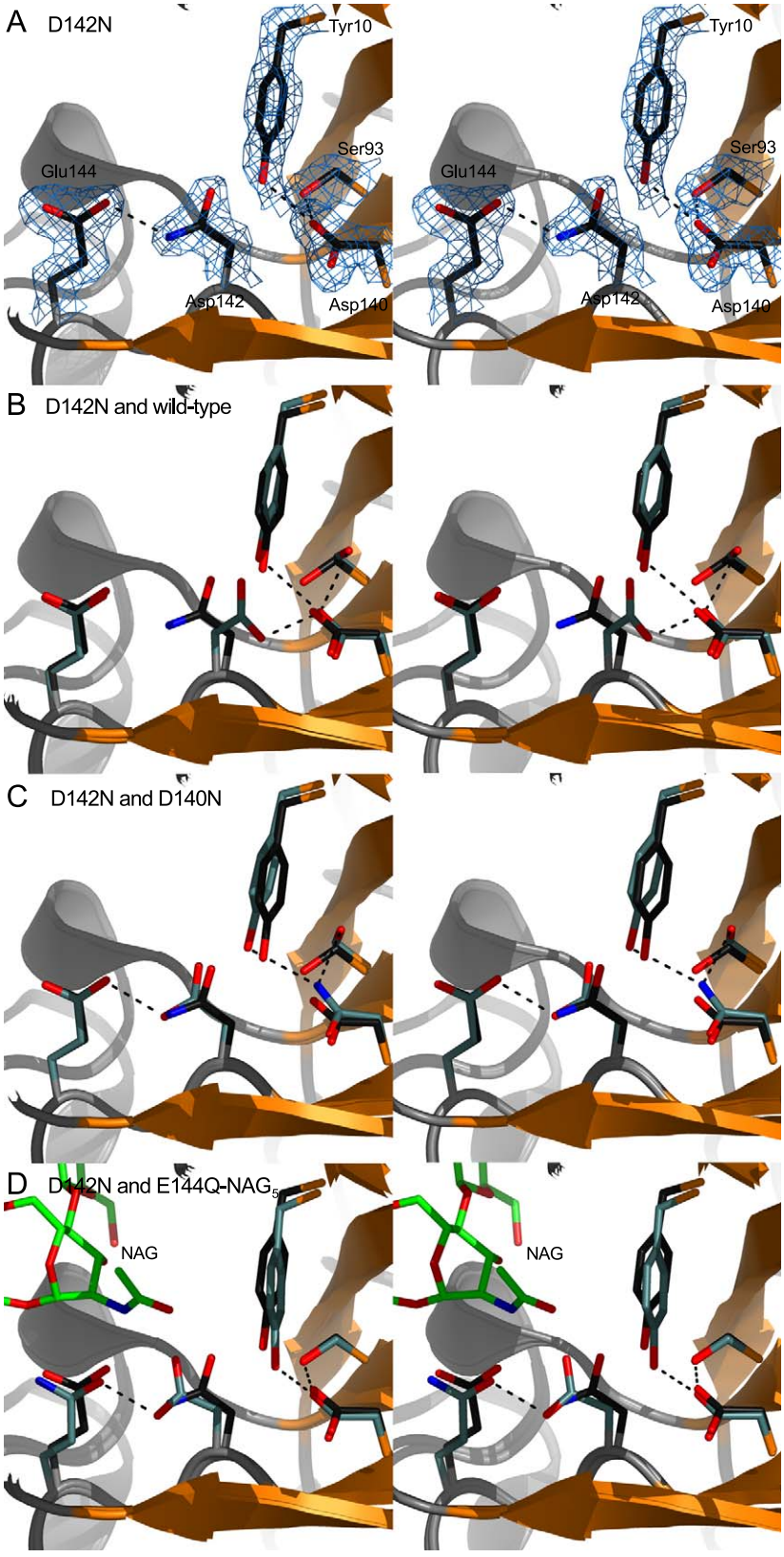
A D142N
Tyr10
Ser93
Glu144
Asp142
Asp140
B D142N and wild-type
C D142N and D140N
D D142N and E144Q-NAG5
NAG

Table 2
Comparison of some important hydrogen bonds in the active site of ChiB[a]

ChiB structure[b]	Tyr10 OH-D140 Oδ2/Nδ2		Ser93 Oγ-Asp/Asn140 Oδ2/Nδ2		Asp142 Oδ1-Asp/Asn140 Oδ2/Nδ2		Asp/Asn142 Oδ2/Nδ2-Glu144 Oε1	
	D–A	HB2	D–A	HB2	D–A	HB2	D–A	HB2
WT	3.2	0.16	2.72	0.61	2.4	0.33	–	–
D140N	3.1	0.67[c]	2.95	0.94[c]	–	–	2.5	0.60
D142N	2.7	0.74	2.71	0.64	–	–	2.6	0.63
E144Q-NAG_5	2.7	0.39	2.74	0.67	–	–	2.6	0.51
WT-allos	2.6	0.45	2.81	0.59	–	–	2.6	0.72
D142N-allos	2.7	0.31	2.81	0.66	–	–	2.8	0.67

Donor–acceptor distances in Å (D–A column) were calculated with WHAT IF [23] using the HB2 algorithm [24], which also determines the geometrical quality of the hydrogen bond given as a numerical value from 0 (no hydrogen bond) to 1 (optimal hydrogen bond) in the HB2 column.

[a] See also Fig. 3.

[b] WT, wild type ChiB ([6]; PDB accession code:1E15); D140N, D140N mutant ([19]; PDB accession code:1GOI); D142N, D142N mutant; E144Q-NAG_5, E144Q mutant of ChiB in complex with NAG_5 ([6]; PDB accession code:1E6N); WT-allos, wild type in complex with allosamidin ([6]; PDB accession code:1E6R); D142N-allos, D142N mutant in complex with allosamidin.

[c] Note that Nδ2 of Asn140 acts as a hydrogen bond donor, whereas the corresponding Oδ2 of Asp140 acts as an acceptor in all other cases.

The structure was similar to the structure of the wild-type apo-enzyme. Superposition of the B monomers yielded an RMSD of 0.484 Å (Cα's only), a value that is dominated by concerted motions of areas peripheral to the active site. Conspicuous differences were observed for several side chain conformations in the active site region (Fig. 3). Compared to Asp142 in the wild-type, the side chain of Asn142 has rotated 90° around χ_1 and is now pointing towards Glu144 instead of Asp140 (Fig. 3B; see Tables 2 and 3 for details on contact analyses and side chain rotations). The Asn142 Nδ2 atom is positioned 2.59 Å away from the Glu144 Oε1 atom, and these two atoms form a hydrogen bond (Fig. 3A, Tables 2 and 3). The position of Asn142 is similar to the position of Asp142 observed in the structures of ChiB in complex with ligands [6,17,27,28]; Fig. 3D). Interestingly, the structure shows other features that have previously been found to be associated with ligand binding: there is a main chain displacement of β-strand 1 in the TIM barrel which brings Tyr10 0.59 Å closer to D140; in addition, the side chain of Ser93 Oγ is rotated by 106° around χ_1 (Fig. 3B,D and Table 3). For comparison, Fig. 3C shows the previously determined structure of the D140N mutant of ChiB [19]. Also in this structure, residue 142 has rotated towards Glu144, but concomitant adjustments of Tyr10 and Ser93 are not observed.

In the A monomer of D142N, Asn142 occurs in both conformations, although primarily in the "up" conformation. Thus, it seems that there is a low barrier between the two conformations of residue D142N.

3.2. The structure of D142N in complex with allosamidin

The structure of the D142N–allosamidin complex was refined to 1.97 Å with *R*-factors converging to $R = 0.188$ and $R_{free} = 0.228$ (Table 1; Fig. 4A). As for most crystal structures of ChiB in complex with a ligand, the side chain of residue 142 (originally an Asp, but in this case an Asn) is pointing towards Glu144 and participates in a hydrogen bond (distance: 2.84 Å; Fig. 4, Table 2). Tyr10 and the side chain of Ser93 have moved in approximately the same way as observed previously in ChiB–ligand complexes and in the D142N mutant (Tables 2 and 3). In terms of position and conformation of allosamidin, the D142N–allosamidin complex is almost indistinguishable from the WT–allosamidin complex (Fig. 4B, RMSD = 0.212 Å). In both cases, allosamidin occupies the −1 to −3 subsites of the catalytic cleft. Thus, the only significant difference between the wild-type and the mutant complex is the chemical nature of residue 142.

3.3. Mutational effects on catalysis and the binding of allosamidin

Kinetic parameters for wild-type ChiB and the D142N mutant are presented in Table 4. The D142N mutant generally displays lower catalytic activity than the wild-type, but the magnitude of the difference varies with pH. For k_{cat}, the reduction varies from a factor 2 at pH 10.0 to a factor 30–60 in the pH 4.2–7.2 interval. The D142N mutant had a 2-fold (at pH 9.0–10.0) to 16-fold (at pH

Fig. 3. Stereo images of the catalytic centres in D142N and other ChiB structures. Protein main chains are shown as cartoons, whereas side chains are shown as sticks. Methyl groups in side chains belonging to D142N are coloured dark grey; methyl groups belonging to other (superposed) structures are coloured light grey. Some relevant contact distances are listed in Table 2. (A) The D142N mutant; side chains are surrounded by the $2|F_o| - |F_c|$, ϕ_{calc} density contoured at 1.5 σ. Hydrogen bonds are shown as dashed black lines. (B) Superposition of D142N and the wild-type (PDB accession code:1E15). The RMSD for the superposition was 0.484 Å. Hydrogen bonds in the wild-type structure are shown as dashed black lines. (C) Superposition of D142N and D140N (PDB accession code:1GOI). The RMSD for the superposition was 0.203 Å. Hydrogen bonds in the D140N structure are shown as dashed black lines. (D) Superposition of the D142N mutant and the E144Q mutant in complex with an *N*-acetylglucosamine pentamer (PDB accession code:1E6N, the sugar carbons are coloured green). The RMSD for the superposition was 0.398 Å. Hydrogen bonds in the E144Q-NAG_5 structure are shown as dashed black lines.

Table 3
Side chain χ_1 angles in the active site of ChiB[a]

ChiB structure[b]	Ser93 χ_1	Asp142/Asn142 χ_1
WT	− 65	− 63
D140N	− 56	− 169
D142N	− 170	− 163
WT-NAG_5	− 179	− 173
WT-allos	− 177	− 182
D142N-allos	− 176	− 183

[a] See also Fig. 3.
[b] See Table 2 for the PDB accession codes.

7.2) lower K_m than the wild-type. Mutating Asp142 to Ala reduced specific activity 1160-fold at most (at pH 6.1).

Table 4 shows that the inhibitory properties of allosamidin are pH-dependent for both WT and D142N. The D142N mutation reduces the affinity for allosamidin at all tested pH values. The lowest affinity for allosamidin and the smallest affinity difference is found at acidic pH.

4. Discussion

The only structural differences between wild-type ChiB and the D142N mutant that seem to affect catalysis concern the position of residue 142 and simultaneous adjustments of Tyr10 and Ser93 (Fig. 3). The adjustments of residues 10 and 93 compensate the charge left on Asp140 when Asp142 rotates towards Glu144 upon substrate binding ([6], Fig. 1). We noted similar structural adjustments in the recently published structure of the D169N mutant of Chitinase 1 from *Coccidioides immitis* ([11]; pdb code1LL6) which corresponds to our D142N mutant. In addition to rotation of residue 169 (as noted by the authors of Ref. [11]), one can observe a displacement of Tyr43 (corresponding to Tyr10 in ChiB) similar to the displacement observed in the D142N structure. Rotation of the residue corresponding to Ser93 in ChiB (S127 in Chitinase 1) is not as pronounced as in D142N but the D169N structure shows an additional rotation (of Thr209, corresponding to Thr184 in ChiB) of a hydroxyl group towards the residue corresponding to Asp140 in ChiB (Asp167 in Chitinase 1). The rotation of Thr209 could be a mechanism for compensation of the charge developing on Asp167 when Asp169 rotates towards Glu171, similar to what is observed for Ser93 in the ChiB structures [6].

The D142N mutant shows an active site conformation that is similar to what is observed in the E144Q mutant of ChiB in complex with substrate (Fig. 3). Thus, the active site seems to be adapted to substrate-binding, which may cause the low K_m of D142N. The D140N mutant is similar

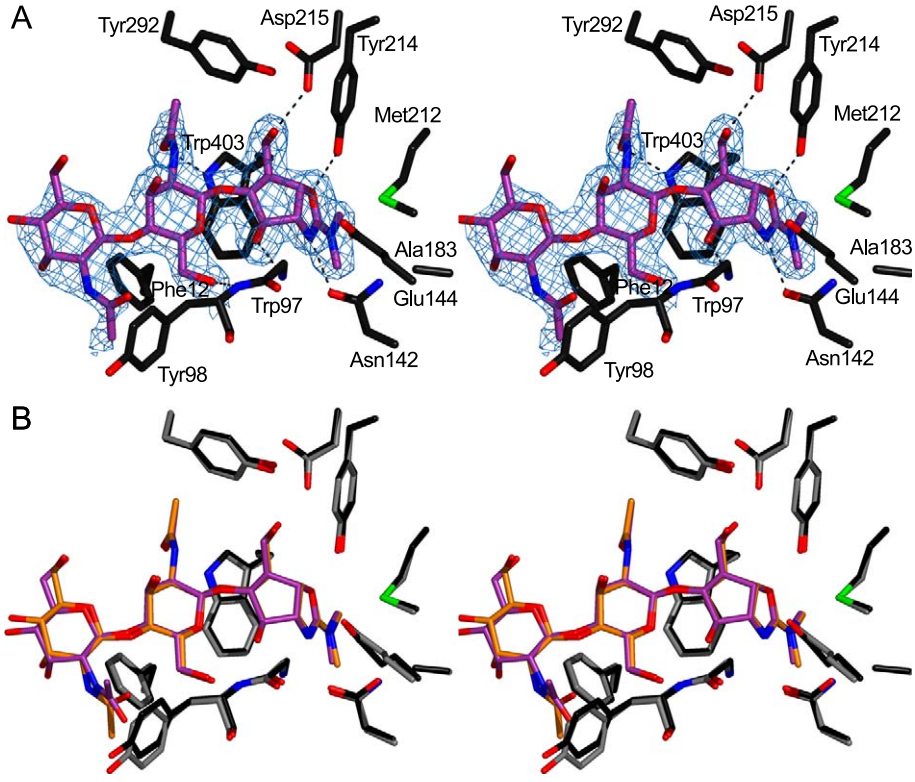

Fig. 4. Stereo images of the D142N–allosamidin complex. (A) Side chains are drawn as sticks in standard colour coding. Allosamidin is drawn in purple sticks surrounded by the unbiased $|F_o| - |F_c|$, ϕ_{calc} density contoured at 2.5 σ. (B). Superposition of the D142N–allosamidin and wild-type–allosamidin complexes (RMSD 0.212 Å). Side chains in wild-type and D142N are drawn in stick representation and are shown in black and grey colour, respectively. Allosamidin is drawn in purple and orange sticks for wild-type and D142N, respectively. For clarity, the side chain of Trp97 is not shown. Figs. 3 and 4 were made using PyMol (www.pymol.org).

Table 4
Kinetic parameters

WT						D142N					D142A
pH	Specific activity[a]	k_{cat} (s^{-1})	K_m (μM)	IC_{50} (μM)	K_i (μM)[b]	Specific activity[a]	k_{cat} (s^{-1})	K_m (μM)	IC_{50} (μM)	K_i (μM)[b]	Specific activity[a]
4.2	1.4×10^2	13 ± 2.3	31 ± 8.2	5.0	3.0	4.2	0.26 ± 0.07	5.4 ± 1.2	1.6×10^2	34	0.13
5.4	1.5×10^2	18 ± 4.5	26 ± 10	2.5	1.4	4.5	0.34 ± 0.05	4.5 ± 2.4	85	15	0.14
6.1	1.5×10^2	18 ± 2.3	31 ± 6.3	0.4	0.2	4.7	0.28 ± 0.04	4.1 ± 2.0	70	12	0.13
7.2	1.2×10^2	17 ± 1.4	38 ± 4.2	0.2	0.1	4.6	0.32 ± 0.05	3.3 ± 2.4	45	6.4	0.14
8.0	57	3.5 ± 1.2	25 ± 13	0.07	0.04	4.0	0.29 ± 0.04	5.7 ± 2.3	18	4.0	0.12
9.0	22	1.2 ± 0.3	46 ± 14	0.08	0.06	3.6	0.31 ± 0.05	17 ± 5.3	8.0	3.7	0.09
10.0	8.0	0.4 ± 0.1	72 ± 23	0.07	0.05	2.0	0.18 ± 0.01	34 ± 3.7	4.0	2.5	0.04

[a] Specific activities (nmol s^{-1} mg^{-1}) are given to enable comparison of WT and D142N with D142A (for which K_m and k_{cat} could not be determined accurately).

[b] K_i values were estimated on the basis of IC_{50} values, in order to obtain a parameter for inhibition that is less influenced by changes in K_m. K_i values were calculated directly from IC_{50} values using the Michaelis–Menten equation for competitive inhibition (which yields $K_i = (K_m \cdot IC_{50})/K_m + [S]$). Note that the K_i values presented should be considered rough estimates.

to the D142N mutant in terms of the position of residue 142 and the removal of one acidic residue in the catalytic centre, but has a 10-fold higher K_m [29] and lacks the adjustments of Ser93 and Tyr10 (Fig. 3, Tables 2 and 3). This may indicate that the additional adjustments of Tyr10 and Ser93 (including some displacement of the backbone around residue 10) are not only important to stabilize Asp140 during the temporary loss of the hydrogen bond with Asp142 (Fig. 1; [6]), but also for effective substrate binding. On the other hand, it should be noted that published K_m effects of mutations analogous to D142N in ChiB vary from a reduction to an increase ([12,14,30,31]; a K_m value for the D169N mutant of Chitinase 1 from *C. immitis* has not yet been published). Such variation is not likely to be explained by assuming changes in the conformations of residues analogous to Tyr10, Ser93, Asp140, Asp142, and Glu144, which are all fully conserved in family 18 chitinases. The variation is more likely to be a result of differences in active site electrostatics (which in principle may be affected by many residues).

The structure of the D142N mutant does not show any clear structural feature that may explain its reduced catalytic activity. In principle it is possible that the enzyme is "locked" in the conformation with Asn142 pointing towards Glu144 and that this is unfavourable for catalysis. This seems not likely though, since Asn142 was observed partially in the "down" conformation in the A monomer. Thus, we conclude that the observed decrease in catalytic activity is primarily due to the difference in electrostatic properties between aspartate and asparagine. It can easily be envisaged that the Asp → Asn mutation leads to poorer stabilization of the transition state of the reaction, which is thought to carry some positive charge [3,4].

To obtain further insights into the role of residue 142 in catalysis, we have studied the interaction of the D142N mutant with allosamidin (Fig. 2). When the ring nitrogen is protonated, the allosamizoline unit looks analogous to the oxazolinium ion intermediate (Fig. 2). Structural analysis of the D142N–allosamidin complex revealed no significant change compared to WT–allosamidin complex, indicating that the changed affinity of the D142N mutant for the inhibitor is solely due to the electrostatic changes in the active site caused by the aspartate to asparagine replacement at position 142.

Binding of allosamidin was found to be pH-dependent, in particular in the pH 4.2–8.0 range (Table 4). Explanation of the pH dependency of allosamidin binding is not straightforward because this dependency reflects the titration of several residues in the active site of the enzyme (Asp142, Glu144; possibly Asp140) and allosamidin itself (Fig. 2; the pK_a of the allosamizoline nitrogen in free allosamidin in solution is approximately 7.5 [32]). In general, allosamidin affinity was more affected by pH in the wild-type than in the D142N mutant. The highest apparent affinity for allosamidin and the largest differences between wild-type and D142N were found at high pH. Together, these observations show that a negative charge on Asp142 contributes dominantly to allosamidin binding, even (or especially) at pH values where free allosamidin may be uncharged (estimated pK_a value 7.5). It is conceivable that the electronegative environment in the enzyme raises the pK_a of bound allosamidin, and that strong electrostatic interactions between the ligand and Asp142 occur due to the fact that they effectively share a proton. The much smaller difference in allosamidin affinity between wild-type and D142N at low pH, probably reflects the fact that Asp142 in the wild-type enzyme is more protonated at these pH values, making its electrostatic properties more similar to those of asparagine.

Interestingly, in the wild-type enzyme, apparent allosamidin affinities are highest at pH values were k_{cat} is lowest. A similar negative correlation is observed in D142N, which still shows considerable pH dependency of allosamidin affinity, while k_{cat} hardly varies with pH. Thus, the ability of the enzyme to stabilize the transition state of the reaction (which is reflected in k_{cat}) is not correlated with its apparent affinity for allosamidin. This is in accordance with the notion that allosamidin is not a transition state analogue,

but rather a structural mimic of the oxazolinium ion intermediate.

Acknowledgements

This work was supported by the Norwegian Research Council grants 140497/420 and 140440/130. DvA is supported by a Wellcome Trust Career Development Research Fellowship. DRH and FR are supported by BBSRC CASE studentships (Cyclacel and Syngenta, respectively). We thank Graham Gooday and Shohei Sakuda for supplying us with allosamidin and Xiaohong Jia and Ellen Hasle Kokkim for technical assistance. We thank the European Synchrotron Facility (Grenoble) for the time at beamline ID14EH1. The coordinates and structure factors have been deposited with the PDB (entries 1OGB and 1OGG).

References

[1] B. Henrissat, G. Davies, Structural and sequence-based classification of glycoside hydrolases, Curr. Opin. Struct. Biol. 7 (1997) 637–644.
[2] K.A. Brameld, W.A. Goddard, Substrate distortion to a boat conformation at subsite −1 is critical in the mechanism of family 18 chitinases, J. Am. Chem. Soc. 120 (1998) 3571–3580.
[3] K.A. Brameld, W.D. Shrader, B. Imperiali, W.A. Goddard, Substrate assistance in the mechanism of family 18 chitinases: theoretical studies of potential intermediates and inhibitors, J. Mol. Biol. 280 (1998) 913–923.
[4] I. Tews, A.C. Terwisscha van Scheltinga, A. Perrakis, K.S. Wilson, B.W. Dijkstra, Substrate-assisted catalysis unifies two families of chitinolytic enzymes, J. Am. Chem. Soc. 119 (1997) 7954–7959.
[5] A.C. Terwisscha van Scheltinga, S. Armand, K.H. Kalk, A. Isogai, B. Henrissat, B.W. Dijkstra, Stereochemistry of chitin hydrolysis by a plant chitinase/lysozyme and X-ray structure of a complex with allosamidin: evidence for substrate assisted catalysis, Biochemistry 34 (1995) 15619–15623.
[6] D.M.F. van Aalten, D. Komander, B. Synstad, S. Gaseidnes, M.G. Peter, V.G.H. Eijsink, Structural insights into the catalytic mechanism of a family 18 exo-chitinase, Proc. Natl. Acad. Sci. U. S. A. 98 (2001) 8979–8984.
[7] M.B. Brurberg, I.F. Nes, V.G.H. Eijsink, Comparative studies of chitinases A and B from *Serratia marcescens*, Microbiology 142 (1996) 1581–1589.
[8] D.M.F. van Aalten, B. Synstad, M.B. Brurberg, E. Hough, B.W. Riise, V.G.H. Eijsink, R.K. Wierenga, Structure of a two-domain chitotriosidase from *Serratia marcescens* at 1.9-A resolution, Proc. Natl. Acad. Sci. U. S. A. 97 (2000) 5842–5847.
[9] B.L. Mark, D.J. Vocadlo, S. Knapp, B.L. Triggs-Raine, S.G. Withers, M.N. James, Crystallographic evidence for substrate-assisted catalysis in a bacterial beta-hexosaminidase, J. Biol. Chem. 276 (2001) 10330–10337.
[10] S.J. Williams, B. Mark, D.J. Vocadlo, M.N. James, S.G. Withers, Aspartate 313 in the *Streptomyces plicatus* hexosaminidase plays a critical role in substrate assisted catalysis by orienting the 2-acetamido group and stabilizing the transition state, J. Biol. Chem. 277 (2002) 40055–40065.
[11] K. Bortone, A.F. Monzingo, S. Ernst, J.D. Robertus, The structure of an allosamidin complex with the *Coccidioides immitis* chitinase defines a role for a second acid residue in substrate-assisted mechanism, J. Mol. Biol. 320 (2002) 293–302.
[12] Y. Papanikolau, G. Prag, G. Tavlas, C.E. Vorgias, A.B. Oppenheim, K. Petratos, High resolution structural analyses of mutant chitinase A complexes with substrates provide new insight into the mechanism of catalysis, Biochemistry 40 (2001) 11338–11343.
[13] Y. Papanikolau, G. Tavlas, C.E. Vorgias, K. Petratos, De novo purification scheme and crystallization conditions yield high-resolution structures of chitinase A and its complex with the inhibitor allosamidin, Acta Crystallogr. 59 (2003) 400–403.
[14] E. Bokma, H.J. Rozeboom, M. Sibbald, B.W. Dijkstra, J.J. Beintema, Expression and characterization of active site mutants of hevamine, a chitinase from the rubber tree *Hevea brasiliensis*, Eur. J. Biochem. 269 (2002) 893–901.
[15] T. Watanabe, Y. Ito, T. Yamada, M. Hashimoto, S. Sekine, H. Tanaka, The roles of the C-terminal domain and type III domains of chitinase A1 from *Bacillus circulans* WL-12 in chitin degradation, J. Bacteriol. 176 (1994) 4465–4472.
[16] S. Sakuda, A. Isogai, S. Matsumoto, A. Suzuki, Search for microbial insect growth regulators: II. Allosamidin, a novel insect chitinase inhibitor, J. Antibiot. (Tokyo) 40 (1987) 296–300.
[17] F.V. Rao, D.R. Houston, R.G. Boot, J.M. Aerts, S. Sakuda, D.M.F. van Aalten, Crystal structures of allosamidin derivatives in complex with human macrophage chitinase, J. Biol. Chem. 278 (2003) 20110–20116.
[18] Z. Otwinowski, W. Minor, Processing of X-ray diffraction data collected in oscillation mode, Methods Enzymol. 276 (1997) 307–326.
[19] G. Kolstad, B. Synstad, V.G.H. Eijsink, D.M.F. van Aalten, Structure of the D140N mutant of chitinase B from *Serratia marcescens* at 1.45 Å resolution, Acta Crystallogr. 58 (2002) 377–379.
[20] T.A. Jones, J.Y. Zou, S.W. Cowan, M. Kjeldgaard, Improved methods for building protein models in electron density maps and the location of errors in these models, Acta Crystallogr. 47 (1991) 110–119.
[21] A.T. Brunger, P.D. Adams, G.M. Clore, W.L. DeLano, P. Gros, R.W. Grosse-Kunstleve, J.S. Jiang, J. Kuszewski, M. Nilges, N.S. Pannu, R.J. Read, L.M. Rice, T. Simonson, G.L. Warren, Crystallography and NMR system: a new software suite for macromolecular structure determination, Acta Crystallogr. 54 (1998) 905–921.
[22] D.M.F. van Aalten, R. Bywater, J.B. Findlay, M. Hendlich, R.W. Hooft, G. Vriend, PRODRG, a program for generating molecular topologies and unique molecular descriptors from coordinates of small molecules, J. Comput. Aided Mol. Des. 10 (1996) 255–262.
[23] G. Vriend, WHAT IF: a molecular modeling and drug design program, J. Mol. Graph. 8 (1990) 52–56.
[24] R.W. Hooft, C. Sander, G. Vriend, Positioning hydrogen atoms by optimizing hydrogen-bond networks in protein structures, Proteins 26 (1996) 363–376.
[25] W. Kabsch, A solution for the best rotation to relate two sets of vectors, Acta. Crystallogr., A 32 (1976) 922–923.
[26] Collaborative Computational Project Number 4, The CCP4 suite: programs for protein crystallography, Acta Crystallogr., D 50 (1994) 760–763.
[27] D.R. Houston, I. Eggleston, B. Synstad, V.G.H. Eijsink, D.M.F. van Aalten, The cyclic dipeptide CI-4 [cyclo-(L-Arg-D-Pro)] inhibits family 18 chitinases by structural mimicry of a reaction intermediate, Biochem. J. 368 (2002) 23–27.
[28] D.R. Houston, K. Shiomi, N. Arai, S. Omura, M.G. Peter, A. Turberg, B. Synstad, V.G.H. Eijsink, D.M.F. van Aalten, High-resolution structures of a chitinase complexed with natural product cyclopentapeptide inhibitors: mimicry of carbohydrate substrate, Proc. Natl. Acad. Sci. U. S. A. 99 (2002) 9127–9132.
[29] B. Synstad, S. Gåseidnes, G. Vriend, J.-E. Nielsen, V.G.H. Eijsink, in: M.G. Peter, R.A.A. Muzzarelli, A. Domard (Eds.), Advances in Chitin Science, vol. 4, Universität Potsdam, Potsdam, 2000, pp. 524–529.

[30] Y. Lu, K.C. Zen, S. Muthukrishnan, K.J. Kramer, Site-directed mutagenesis and functional analysis of active site acidic amino acid residues D142, D144 and E146 in *Manduca sexta* (tobacco hornworm) chitinase, Insect Biochem. Mol. Biol. 32 (2002) 1369–1382.
[31] T. Watanabe, M. Uchida, K. Kobori, H. Tanaka, Site-directed mutagenesis of the Asp-197 and Asp-202 residues in chitinase A1 of *Bacillus circulans* WL-12, Biosci. Biotechnol. Biochem. 58 (1994) 2283–2285.
[32] J. Pitha, J. Jonas, J. Kovar, K. Blaha, Zur Konfiguration Stickstoffhaltiger Verbindungen: 13. Uber Die Darstellung Und Tautomerie Der Aminooxazoline, Collection of Czechoslovak Chemical Communications 26 (1961) 834–846.